J. Fluid Mech. (1969), *vol.* 38, *part* 1, *pp.* 75–96
Printed in Great Britain

Viscous flow in a cylindrical tube containing a line of spherical particles

By HENRY WANG† AND RICHARD SKALAK

Department of Civil Engineering and Engineering Mechanics,
Columbia University, New York

(Received 3 September 1968 and in revised form 14 November 1968)

The viscous, creeping flow through a cylindrical tube of a liquid, which contains rigid, spherical particles, is investigated analytically. The spheres are located on the axis of the cylinder and are equally spaced. Solutions are derived for particles in motion and fixed, with and without fluid discharge. Numerical results are presented for the drag on each sphere and the mean pressure drop for a wide range of sizes and spacings of the spheres. The study is motivated by possible application to blood flow in capillaries, where red blood cells represent particles of the same order of magnitude as the diameter of the capillary itself. The results may also be of interest in other applications, such as sedimentation and fluidized beds. It is shown that there is little interaction between particles if the spacing is more than one tube diameter, and that the additional pressure drop over that for Poiseuille flow is less than 50 % if the sphere diameter is less than 0·8 of the tube diameter.

1. Introduction

The present study was motivated by the possible application of the results to blood flow in capillary blood vessels, in which the red blood cells represent particles whose diameter is of the same order of magnitude as the diameter of the blood vessel itself. Red blood cells are flexible, biconcave disks, but to permit analytic treatment they are herein approximated by rigid spheres.

In the idealized problem considered (see figure 1), an infinite row of rigid spheres is assumed to be moving in a viscous, incompressible fluid bounded by a fixed circular cylinder. The spheres are equally spaced along the axis of the cylinder, and the Reynolds number is assumed to be so low that inertial terms may be neglected.

It can be shown that, for creeping flow, the fluid motion for the geometry shown in figure 1 is unique for a given velocity of the spheres, U, and a given discharge, Q (Wang & Skalak 1967). Solutions are derived below for arbitrary U and Q, but three subcases are of interest: (i) $U = 0$, $Q \neq 0$, which represents flow in a cylindrical tube containing spheres which are each fixed in position; (ii) $U \neq 0$, $Q = 0$, which represents a line of spheres moving in a fluid otherwise at rest as in the case of particles settling in a cylinder of fluid; (iii) the case of

† Now at the Naval Ship Research and Development Center, Washington, D.C.

zero drag on each particle, which is achieved if the fluid and particles are being pumped steadily through the tube by a pressure gradient, as is the case in blood flow.

In cases (i) and (ii), the drag on each particle is different from zero, and there is also a mean pressure gradient along the cylinder. By superimposing the two cases of non-zero drag in proper proportion, a net drag equal to zero can be achieved. Numerical results are given below for all three cases.

Previous investigators have considered the influence of a cylindrical wall on the drag exerted on a single sphere (Haberman & Sayre 1958), but no comparable results are available for an infinite line of spheres. A general discussion and some numerical results were given by Sonshine & Brenner (1966). The present paper gives numerical results for pressure drop and drag for a range of the ratio, λ, of the sphere radius to the tube radius of $0 < \lambda \leqslant 0{\cdot}9$, and a range of sphere spacing from the case of adjacent spheres touching up to a maximum spacing of forty tube radii. The present paper is complementary to Lighthill (1968), which considers elastic particles that nearly fit the tube, using lubrication theory.

The analytic techniques used in the present paper were suggested by the work of Ling (1963) and Atsumi (1960) on problems in the theory of elasticity involving similar geometry, e.g. torsion and tension of a circular bar containing an infinite row of spherical cavities.

2. Formulation

The flows of interest are assumed to be axisymmetric, so that a Stokes stream function exists. It is convenient to work in terms of dimensionless (unprimed) co-ordinates, which are defined in terms of the dimensional (primed) co-ordinates (figure 1) by

$$R = R'/a, \quad z = z'/a, \quad r = r'/a, \tag{2.1}$$

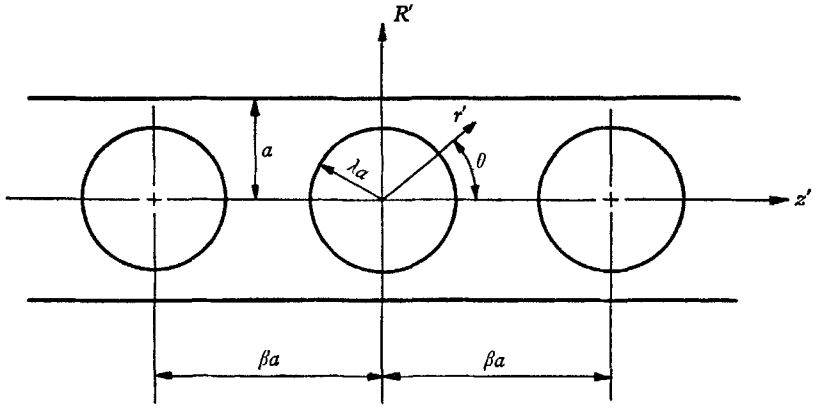

FIGURE 1. Geometry of the problem.

where a is the radius of the cylinder, (R', z') are cylindrical co-ordinates, and (r', θ) are spherical co-ordinates. We assume that the body force, if any, is a constant, g, per unit mass, and that it acts only in the axial direction, $+z$. If the

body force acts in a direction other than the axial direction, then the particles must be neutrally buoyant in order to remain concentric in the cylinder. The present analysis can be applied to this case by setting $g = 0$.

The dependent variables of interest are the velocity, $\mathbf{V}'$, pressure, p', stress tensor, τ'_{ij}, Stokes stream function, ψ', drag D', and discharge, Q'. These are expressed in dimensionless form, using the fluid density and kinematic viscosity, ρ and ν, and the tube radius, a, as follows:

$$\left.\begin{aligned} &\mathbf{V} = a\mathbf{V}'/\nu, \quad p = \frac{p'a^2}{\rho\nu^2} - \frac{a^2 g z'}{\nu^2}, \quad \tau_{ij} = \tau'_{ij}a^2/\rho\nu^2, \\ &D = D'/\rho\nu^2, \quad \psi = \psi'/a\nu, \quad Q = Q'/a\nu. \end{aligned}\right\} \tag{2.2}$$

In (2.2) the effect of the body force is incorporated in the dimensionless pressure. Then the equations of motion and continuity are

$$-\nabla p + \nabla^2 \mathbf{V} = 0, \tag{2.3}$$

$$\nabla . \mathbf{V} = 0, \tag{2.4}$$

where ∇ is the gradient operator in dimensionless co-ordinates. Taking the curl of (2.3) gives

$$\nabla^2 \boldsymbol{\zeta} = 0, \tag{2.5}$$

where $\boldsymbol{\zeta}$ is the dimensionless vorticity, $\nabla \times \mathbf{V}$. Equation (2.5) yields a fourth-order equation, $L^4\psi = 0$, for axisymmetric flow. In cylindrical co-ordinates (Happel & Brenner 1965),

$$\left[\frac{\partial^2}{\partial z^2} + \frac{\partial^2}{\partial R^2} - \frac{1}{R}\frac{\partial}{\partial R}\right]^2 \psi(z, R) = 0, \tag{2.6}$$

and the velocity components are

$$v_z = -\frac{1}{R}\frac{\partial \psi}{\partial R}, \quad v_R = \frac{1}{R}\frac{\partial \psi}{\partial z}. \tag{2.7}$$

In spherical co-ordinates, $L^4\psi = 0$ is (Happel & Brenner 1965)

$$\left[\frac{\partial^2}{\partial r^2} + \frac{1-\cos^2\theta}{r^2}\frac{\partial^2}{\partial(\cos\theta)^2}\right]^2 \psi(r, \theta) = 0, \tag{2.8}$$

and the velocity components are

$$v_r = -\frac{1}{r^2 \sin\theta}\frac{\partial \psi}{\partial \theta}, \quad v_\theta = \frac{1}{r \sin\theta}\frac{\partial \psi}{\partial r}. \tag{2.9}$$

The general problem considered is to find the stream function, ψ, for arbitrary sphere velocity, U, and discharge, Q (figure 1). The discharge, Q, is computed on any cross-section of the tube and includes both the solid and liquid components. In terms of the stream function, Q is given by

$$Q = -2\pi[\psi]_{R=1}, \tag{2.10}$$

where it assumed that ψ is adjusted so that $[\psi]_{R=0} = 0$.

The boundary conditions to be satisfied by ψ are as follows: at the cylinder walls, $R = 1$,

$$\psi = -\frac{Q}{2\pi} \quad v_z = 0; \tag{2.11}$$

on the spherical surfaces, $r_n = \lambda$, $n = 0, \pm 1, \pm 2, \ldots$,

$$v_z = U, \quad v_R = 0, \tag{2.12}$$

where

$$r_n = [R^2 + (z - n\beta)^2]^{\frac{1}{2}}, \tag{2.13}$$

and λ and β are the dimensionless radius and spacing of the spheres (figure 1). The above boundary conditions apply in a co-ordinate system fixed with respect to the tube wall. It is convenient to use instead a co-ordinate system fixed with respect to the spheres in which the boundary conditions are as follows:
at the cylinder walls, $R = 1$,

$$\psi = -\frac{Q}{2\pi} + \frac{U}{2}, \quad v_z = -U; \tag{2.14}$$

on the spherical surfaces, $r_n = \lambda$,

$$\psi = 0, \quad \frac{\partial \psi}{\partial r_n} = 0. \tag{2.15}$$

In (2.14) and below, Q and U are the discharge and sphere velocity in co-ordinates fixed with respect to the tube wall. The stream function, ψ, is written for co-ordinates moving with the spheres. Now let

$$\psi = \psi_0 + \psi_a, \tag{2.16}$$

where ψ_0 is the Poiseuille flow that would take place if there were no spheres present;

$$\psi_0 = \left(\frac{U}{2} - \frac{V}{2}\right) R^2 + \frac{V}{4} R^4, \tag{2.17}$$

where

$$V = \frac{2Q}{\pi}. \tag{2.18}$$

The boundary conditions on the additional stream function, ψ_a, are then:
at the cylinder walls, $R = 1$,

$$v_z = -\frac{1}{R}\frac{\partial \psi_a}{\partial R} = 0, \quad \psi_a = 0; \tag{2.19}$$

on the spherical surfaces, $r_n = \lambda$,

$$\psi_a = -\psi_0, \quad \frac{\partial \psi_a}{\partial r_n} = -\frac{\partial \psi_0}{\partial r_n}. \tag{2.20}$$

The problem is now to find a ψ_a which satisfies $L^4 \psi_a = 0$ and the boundary conditions (2.19) and (2.20).

3. Solution for ψ

Solutions to $L^4 \psi = 0$ which are useful in the present case are given by Haberman & Sayre (1958). Solutions in cylindrical co-ordinates, which are even and periodic in z, with period β, and which give finite velocities everywhere, are

$$\psi(z, R) = A_0 R^4 + B_0 R^2 + \sum_{m=1}^{\infty} [A_m R I_1(mKR) + B_m R^2 I_0(mKR)] \cos mKz, \tag{3.1}$$

where $K = 2\pi/\beta$ and I_1 and I_0 are modified Bessel functions of the first kind. A_m, B_m are arbitrary constants.

Solutions in spherical co-ordinates, which are even in z and give rise to finite velocities everywhere, except possibly at infinity and at the origin, are

$$\psi(r,\theta) = \sum_{n=2}^{\infty} C_n^{-\frac{1}{2}}(\cos\theta)\,[A_n r^n + B_n r^{-n+1} + C_n r^{n+2} + D_n r^{-n+3}], \tag{3.2}$$

where $n = 2, 4, 6, \ldots$, and $C_n^{-\frac{1}{2}}(\cos\theta)$ are Gegenbauer functions of order n and degree $-\frac{1}{2}$. A_n, B_n, C_n, D_n are arbitrary constants. The present problem requires solutions which are periodic as well as even in z. Periodic functions in spherical co-ordinates can be constructed by replacing z in (3.2) by $(z-n\beta)$ and summing over n from $-\infty$ to $+\infty$. Physically, this corresponds to placing appropriate singularities at the centre of each sphere in figure 1. The following two even, periodic solutions are constructed in this way:

$$\psi^{(1)} = \sum_{n=-\infty}^{\infty} \frac{R^2}{2[R^2+(z-n\beta)^2]^{\frac{1}{2}}} + \{A_0 R^4 + B_0 R^2 + \sum_{m=1}^{\infty} [A_m R I_1(mKR) + B_m R^2 I_0(mKR)]\cos mKz\}, \tag{3.3}$$

$$\Psi^{(2)} = \left\{\frac{1}{2}\frac{R^2}{[R^2+z^2]^{\frac{1}{2}}} + \frac{1}{2}\sum_{n=1}^{\infty}\left[\frac{R^2}{[R^2+(z-n\beta)^2]^{\frac{1}{2}}} + \frac{R^2}{[R^2+(z+n\beta)^2]^{\frac{1}{2}}} - \frac{2R^2}{n\beta}\right]\right\} + \left\{C_0 R^4 + D_0 R^2 + \sum_{m=1}^{\infty}[C_m R I_1(mKR) + D_m R^2 I_0(mKR)]\cos mKz\right\}, \tag{3.4}$$

where A_m, B_m, C_m, and D_m are arbitrary constants. The portions of the solutions containing these constants will be used to satisfy the boundary conditions on the cylindrical wall.

The first term of $\psi^{(1)}$ comes from $C_2^{-\frac{1}{2}}(\cos\theta)r^{-2+1} = R^2/2r^3$, and the first term of $\psi^{(2)}$ comes from $C_2^{-\frac{1}{2}}(\cos\theta)r^{-2+3} = R^2/2r$. These two terms may be regarded as the terms which occur in the Stokes solution for a single sphere in an infinite fluid.

The functions $\psi^{(1)}$ and $\psi^{(2)}$ are now adjusted so that each satisfies the boundary conditions at the cylindrical wall,

$$\psi = v_z = 0 \quad \text{on} \quad R = 1. \tag{3.5}$$

For $\psi^{(1)}$, the boundary conditions (3.5) require:

$$\text{for} \quad \psi = 0\text{:}\quad A_0 + B_0 + \sum_{m=1}^{\infty}[A_m I_1(mK) + B_m I_0(mK)]\cos mKz,$$

$$= -\sum_{n=-\infty}^{\infty}\frac{1}{2[1+(z-n\beta)^2]^{\frac{3}{2}}}; \tag{3.6}$$

$$\text{for} \quad v_z = 0\text{:}\quad 4A_0 + 2B_0 + \sum_{m=1}^{\infty}[A_m mK I_0(mK) + B_m(2I_0(mK) + mK I_1(mK))]\cos mKz,$$

$$= -\left\{\sum_{n=-\infty}^{\infty}\frac{1}{[1+(z-n\beta)^2]^{\frac{5}{2}}} - \frac{3}{2}\frac{1}{[1+(z-n\beta)^2]^{\frac{3}{2}}}\right\}. \tag{3.7}$$

Both sides of (3.6) and (3.7) are multiplied by $\cos mKz$ and then integrated from $-\frac{1}{2}\beta$ to $\frac{1}{2}\beta$, to derive a pair of algebraic equations for each pair of the A_m, B_m, $m = 0, 1, 2, 3, \ldots$. A similar set of equations for each of the pairs C_m, D_m is derived by applying (3.5) to $\psi^{(2)}$. The following results are obtained by solving the several sets simultaneously:

$$\left.\begin{aligned} A_m &= \frac{2}{\beta}\frac{(mK)^2[I_1(mK)K_1(mK)+I_0(mK)K_2(mK)]}{mK[I_0^2(mK)-I_1^2(mK)]-2I_0(mK)I_1(mK)}, \\ B_m &= \frac{2}{\beta}\frac{(mK)^2[-I_0(mK)K_1(mK)-I_1(mK)K_2(mK)]+2mKI_1(mK)K_1(mK)}{mK[I_0^2(mK)-I_1^2(mK)]-2I_0(mK)I_1(mK)}, \\ A_0 &= \frac{1}{\beta}, \quad B_0 = \frac{-2}{\beta}, \quad C_m = -\frac{B_m}{mK}; \end{aligned}\right\} \tag{3.8}$$

$$\left.\begin{aligned} D_m = \frac{2}{\beta}\{&(mK)[-I_0(mK)K_2(mK)-I_1(mK)K_1(mK)]+[2I_0(mK)K_1(mK) \\ &+2K_0(mK)I_1(mK)]\}/\{(mK)[I_0^2(mK)-I_1^2(mK)]-2I_0[mK)I_1(mK)]\}, \\ C_0 = \frac{1}{2\beta}, \quad D_0 &= \frac{1}{2\beta}\{-2\log(2\beta)+2E-1\}, \end{aligned}\right\} \tag{3.9}$$

where Euler's constant

$$E = \lim_{N\to\infty}\left[\sum_{n=1}^{N}\frac{1}{n}-\log N\right] = 0{\cdot}577215665. \tag{3.10}$$

The modified Bessel functions of the second kind, K_n, which occur in (3.8) and (3.9) arise from the integrals with respect to z (see Watson 1944, p. 185).

Next, we note that even derivatives of $\psi^{(1)}$ and $\psi^{(2)}$ with respect to z generate additional functions, each of which satisfies $L^4\psi = 0$ and the boundary conditions (3.5) at $R = 1$. They are also periodic and even in z. Hence, we define

$$\psi_{2s}^{(i)} = \frac{1}{(2s-2)!}\frac{\partial^{2s-2}\psi^{(i)}}{\partial z^{2s-2}} \quad (s \geqslant 1,\ i = 1, 2). \tag{3.11}$$

The differentiations called for in (3.11) generate a complete set of functions, which contain singularities of all the even orders n in (3.2). The stream function ψ_a is assumed to be of the form

$$\psi_a = \sum_{s=1}^{\infty}[E_{2s}\psi_{2s}^{(1)}+F_{2s}\psi_{2s}^{(2)}]. \tag{3.12}$$

The constants E_{2s} and F_{2s} in (3.12) are to be determined so that the boundary conditions (2.20) on the spherical surfaces are satisfied. For this purpose, the functions defined by (3.11) are expressed in spherical co-ordinates. This is a critical and important step of the entire procedure. As an example of the procedure, consider the first series in (3.4), which may be written in the form

$$\sum_{n=-\infty}^{\infty}\frac{R^2}{2[R^2+(z-n\beta)^2]^{\frac{3}{2}}} = \frac{R^2}{2r^3}+\sum_{n=1}^{\infty}\frac{R^2}{2(n\beta)^3[1+2h_n\mu+h_n^2]^{\frac{3}{2}}} + \sum_{n=1}^{\infty}\frac{R^2}{2(n\beta)^3[1-2h_n\mu+h_n^2]^{\frac{3}{2}}}, \tag{3.13}$$

where $\mu = \cos\theta$ and $h_n = r/n\beta$. The sums on the right-hand side of (3.13) are recognized in terms of Legendre functions using the relations (Hobson 1955, pp. 105, 107):

$$\frac{1.3.5\ldots(2m-1)h^m}{(1-2h\mu+h^2)^{m+\frac{1}{2}}} = \sum_{n=m}^{\infty} h^n \frac{d^m P_n(\mu)}{d\mu^m}, \tag{3.14}$$

$$(-1)^m (1-\mu^2)^{\frac{1}{2}m} \frac{d^m P_n(\mu)}{d\mu^m} = P_n^m(\mu), \tag{3.15}$$

where P_n are Legendre polynomials of nth degree, and P_n^m are associated Legendre functions of the mth order and nth degree. Using (3.14) and (3.15), equation (3.13) becomes

$$\sum_{n=-\infty}^{\infty} \frac{R^2}{2[R^2+(z-n\beta)^2]^{\frac{3}{2}}} = \frac{R^2}{2r^3} - \tfrac{1}{2}R \sum_{n=1}^{\infty}\sum_{q=0}^{\infty} \frac{(-1)^q r^{q+1}}{(n\beta)^{q+3}} P_{1+q}^1(\cos\theta) - \tfrac{1}{2}R \sum_{n=1}^{\infty}\sum_{q=0}^{\infty} \frac{r^{q+1}}{(n\beta)^{q+3}} P_{1+q}^1(\cos\theta). \tag{3.16}$$

The derivatives with respect to z of (3.16) are also required, and they are found using known recurrence relations (Hobson 1955; pp. 105, 138). The end result is

$$\frac{\partial^{2s-2}}{\partial z^{2s-2}} \sum_{n=-\infty}^{\infty} \frac{R^2}{2[R^2+(z-n\beta)^2]^{\frac{3}{2}}} = -\frac{R}{2}\frac{(2s-2)!}{r^{2s}} P_{2s-1}^1(\cos\theta) - R \sum_{n=1}^{\infty}\sum_{l=0}^{\infty} \frac{1}{(n\beta)^{2l+2s+1}} \frac{(2l+2s)!}{(2l+2)!} r^{2l+1} P_{2l+1}^1(\cos\theta). \tag{3.17}$$

The terms containing I_0 and I_1 in (3.3) and (3.4) must also be converted to spherical co-ordinates. The key relation used for this purpose is (MacRobert 1948, p. 109)

$$\sum_{n=0}^{\infty} \frac{R^n}{n!} P_n(\cos\theta) = e^x J_0(y), \tag{3.18}$$

where $x = R\cos\theta$ and $y = R\sin\theta$. Equation (3.18) and the two relations

$$I_\nu(z) = e^{-\nu\pi i/2} J_\nu(iz), \tag{3.19}$$

$$\sin\theta P_{2n} = -\frac{P_{2n+1}^1}{4n+1} + \frac{P_{2n-1}^1}{4n+1} \tag{3.20}$$

are used to arrive at

$$\frac{\partial^{2s-2}}{\partial z^{2s-2}}[R^2 I_0(mKR)\cos mKz] = R \sum_{l=0}^{\infty} \left\{ \frac{(-1)^{l+s}(mK)^{2l+2s-2}}{(2l+2)!} r^{2l+1} \left[\frac{(2l+2)(2l+1)}{4l+1} + \frac{(mK)^2 r^2}{4l+5} \right] P_{2l+1}^1 \right\}. \tag{3.21}$$

Since $I_1(x) = (d/dx)I_0(x)$, equation (3.21) can also be used to derive

$$\frac{\partial^{2s-2}}{\partial z^{2s-2}}[RI_1(mKR)\cos mKz] = R \sum_{l=0}^{\infty} \frac{(-1)^{l+s}(mK)^{2l+2s-1}}{(2l+2)!} r^{2l+1} P_{2l+1}^1. \tag{3.22}$$

The sum of (3.17), (3.21) and (3.22) expresses $\psi_{2s}^{(1)}$ in spherical co-ordinates. Similar procedures are used to convert $\psi_{2s}^{(2)}$ to spherical co-ordinates. Finally, ψ_0, equation (2.17), is expressed in spherical co-ordinates as

$$\psi_0 = R\left\{P_1^1\left[\left(-\frac{U}{2}+\frac{V}{2}\right)r-\frac{Vr^3}{5}\right]+P_3^1\frac{Vr^3}{30}\right\}. \tag{3.23}$$

In spherical co-ordinates, the complete stream function, ψ, is

$$\begin{aligned}\psi = \psi_a+\psi_0 = \sin\theta\Bigg[&\sum_{s=1}^{\infty}F_{2s}\Bigg\{\frac{1}{2(4s-3)}\frac{1}{r^{2s-3}}(P_{2s-3}^1-P_{2s-1}^1)\\
&+\delta_{1s}\left[-\frac{r^2}{2\beta}(-2\log(2\beta)+2E-1)P_1^1+\frac{r^4}{2\beta}(-\tfrac{4}{5}P_1^1+\tfrac{4}{30}P_3^1)\right]\\
&+\sum_{l=0}^{\infty}[r^{2l+2}(-\tau_{2s}^{2l}+(\beta_2)_{2s}^{2l}+(\gamma_2)_{2s}^{2l})+r^{2l+4}(\xi_{2s}^{2l}+(\sigma_2)_{2s}^{2l})]P_{2l+1}^1\Bigg\}\\
&+\sum_{s=1}^{\infty}E_{2s}\Bigg\{\frac{-1}{2r^{2s-1}}P_{2s-1}^1+\delta_{1s}\left[\frac{2}{\beta}r^2P_1^1+\frac{1}{\beta}r^4(-\tfrac{4}{5}P_1^1+\tfrac{4}{30}P_3^1)\right]\\
&+\sum_{l=0}^{\infty}[r^{2l+2}(-\alpha_{2s}^{2l}+(\beta_1)_{2s}^{2l}+(\gamma_1)_{2s}^{2l})+r^{2l+4}(\sigma_1)_{2s}^{2l}]P_{2l+1}^1\Bigg\}\\
&+\left\{P_1^1\left[\left(\frac{V}{2}-\frac{U}{2}\right)r^2-\frac{Vr^4}{5}\right]+P_3^1\frac{Vr^4}{30}\right\}\Bigg],\end{aligned} \tag{3.24}$$

where

$$\left.\begin{aligned}\tau_{2s}^{2l} &= \sum_{n=1}^{\infty}\frac{1}{(n\beta)^{2l+2s-1}}\frac{(2l+2s-2)!}{(2s-2)!\,(2l)!}\frac{1}{4l+1},\\
\xi_{2s}^{2l} &= \sum_{n=1}^{\infty}\frac{1}{(n\beta)^{2l+2s+1}}\frac{(2l+2s)!}{(2s-2)!\,(2l+2)!}\frac{1}{4l+5},\\
(\beta_2)_{2s}^{2l} &= \sum_{m=1}^{\infty}C_m\frac{(-1)^{l+s}(mK)^{2l+2s-1}}{(2l+2)!\,(2s-2)!},\\
(\gamma_2)_{2s}^{2l} &= \sum_{m=1}^{\infty}D_m\frac{(-1)^{l+s}(mK)^{2l+2s-2}}{(2l)!\,(2s-2)!\,(4l+1)},\\
(\sigma_2)_{2s}^{2l} &= \sum_{m=1}^{\infty}D_m\frac{(-1)^{l+s}(mK)^{2l+2s}}{(2l+2)!\,(2s-2)!\,(4l+5)},\\
\alpha_{2s}^{2l} &= \sum_{n=1}^{\infty}\frac{1}{(n\beta)^{2l+2s+1}}\frac{(2l+2s)!}{(2l+2)!\,(2s-2)!},\\
(\beta_1)_{2s}^{2l} &= \sum_{m=1}^{\infty}A_m\frac{(-1)^{l+s}(mK)^{2l+2s-1}}{(2l+2)!\,(2s-2)!},\\
(\gamma_1)_{2s}^{2l} &= \sum_{m=1}^{\infty}B_m\frac{(-1)^{l+s}(mK)^{2l+2s-2}}{(2l)!\,(2s-2)!\,(4l+1)},\\
(\sigma_1)_{2s}^{2l} &= \sum_{m=1}^{\infty}B_m\frac{(-1)^{l+s}(mK)^{2l+2s}}{(2l+2)!\,(2s-2)!\,(4l+5)}.\end{aligned}\right\} \tag{3.25}$$

Each of the formulas in (3.25) holds for $s = 1, 2, 3, \ldots$ and $l = 0, 1, 2, \ldots$ with the one exception that for $s = 1$ and $l = 0$

$$\tau_{2s}^{2l} = 0. \tag{3.26}$$

It remains to satisfy the boundary conditions (2.15) on the surface of each sphere. Since ψ is periodic in z, it suffices to satisfy (2.15) on the sphere centred at the origin. This leads to two equations, each of which is a linear sum of the functions $P^1_{2l+1}(l = 0, 1, 2, \ldots)$. Since the P^1_{2l+1} form a linearly independent set, the zero boundary conditions (2.15) require the coefficient of each P^1_{2l+1} to be zero. This yields two infinite sets of linear, algebraic equations on the coefficients E_{2s} and F_{2s}, which may be written in the form

$$
\begin{aligned}
&-\frac{F_{2l+2}}{4l+1}+F_2\left\{\left[-\frac{3\lambda}{2\beta}(-2\log(2\beta)+2E-1)-\frac{2\lambda^3}{\beta}\right]\delta_{0l}+\frac{28}{60\beta}\lambda^5\delta_{1l}\right\}\\
&\quad+E_2\left\{\left(\frac{6\lambda}{\beta}-\frac{4\lambda^3}{\beta}\right)\delta_{0l}+\frac{28}{30\beta}\lambda^5\delta_{1l}\right\}\\
&\quad+\sum_{s=1}^{\infty}\{F_{2s}[(4l+3)(-\tau_{2s}^{2l}+(\beta_2)_{2s}^{2l}+(\gamma_2)_{2s}^{2l})\lambda^{4l+1}+(4l+5)(\xi_{2s}^{2l}+(\sigma_2)_{2s}^{2l})\lambda^{4l+3}]\\
&\quad+E_{2s}[(4l+3)(-\alpha_{2s}^{2l}+(\beta_1)_{2s}^{2l}+(\gamma_1)_{2s}^{2l})\lambda^{4l+1}+(4l+5)(\sigma_1)_{2s}^{2l}\lambda^{4l+3}]\}\\
&\qquad=U\tfrac{3}{2}\lambda\delta_{0l}+V\{(-\tfrac{3}{2}\lambda+\lambda^3)\delta_{0l}-\tfrac{7}{30}\lambda^5\delta_{1l}\},
\end{aligned}
\tag{3.27}
$$

$$
\begin{aligned}
&-\frac{F_{2l+4}}{4l+5}+E_{2l+2}+F_2\left\{\left[-\frac{\lambda^3}{2\beta}(-2\log(2\beta)+2E-1)-\frac{12}{10}\frac{\lambda^5}{\beta}\right]\delta_{0l}+\frac{1}{3\beta}\lambda^7\delta_{1l}\right\}\\
&\quad+E_2\left\{\left(\frac{2\lambda^3}{\beta}-\frac{12}{5\beta}\lambda^5\right)\delta_{0l}+\frac{2}{3\beta}\lambda^7\delta_{1l}\right\}\\
&\quad+\sum_{s=1}^{\infty}\{F_{2s}[(4l+1)(-\tau_{2s}^{2l}+(\beta_2)_{2s}^{2l}+(\gamma_2)_{2s}^{2l})\lambda^{4l+3}+(4l+3)(\xi_{2s}^{2l}+(\sigma_2)_{2s}^{2l})\lambda^{4l+5}]\\
&\quad+E_{2s}[(4l+1)(-\alpha_{2s}^{2l}+(\beta_1)_{2s}^{2l}+(\gamma_1)_{2s}^{2l})\lambda^{4l+3}+(4l+3)(\sigma_1)_{2s}^{2l}\lambda^{4l+5}]\}\\
&\qquad=\frac{U}{2}\lambda^3\delta_{0l}+V\left\{\left(-\tfrac{1}{2}\lambda^3+\frac{3\lambda^5}{5}\right)\delta_{0l}-\frac{5\lambda^7}{30}\delta_{1l}\right\}.
\end{aligned}
\tag{3.28}
$$

The two sets of equations (3.27) and (3.28) were solved simultaneously by successive approximations. Both sets were truncated, so that the combined sets contained the same number of equations as unknowns starting from a 2×2 matrix up to a maximum of 16×16.

4. Drag and pressure drop

Once the coefficients E_{2s} and F_{2s} are computed, the stream function is completely determined, and the physical quantities of interest, such as drag and pressure drop, can be computed. Since each sphere is moving at a constant velocity, the equation of motion requires that the sum of all the forces on each sphere be zero. For the typical sphere centred at the origin, the sum of the forces, F_t, in dimensionless form, is

$$
F_t = F_e + W_s + 2\pi\lambda^2\int_0^{\pi}(\tau_{rr}\cos\theta-\tau_{r\theta}\sin\theta)\sin\theta\,d\theta = 0, \tag{4.1}
$$

where $F_e = F'_e/\rho v^2$ and F'_e is the applied external force on each particle. $W_s = W'_s/\rho v^2$ and W'_s is the weight of the particle. The integral term in (4.1)

includes both the drag, D, due to the viscosity of the fluid, and the buoyant effect of the fluid. The stress components in (4.1) are

$$\tau_{rr} = -p + 2\frac{\partial v_r}{\partial r} + gz\frac{a^3}{\nu^2}, \tag{4.2}$$

$$\tau_{r\theta} = \frac{1}{r}\frac{\partial v_r}{\partial \theta} - \frac{v_\theta}{r} + \frac{\partial v_\theta}{\partial r}. \tag{4.3}$$

$\tau_{r\theta}$ is evaluated from (4.3), (3.24) and (2.9), and recurrence relations:

$$\begin{aligned}
\tau_{r\theta} = \sum_{s=1}^{\infty} F_{2s}\Bigg\{ & -\frac{2(2s)(s-1)}{(4s-3)r^{2s}} P^1_{2s-1} + \frac{(2s-1)(2s-3)}{(4s-3)r^{2s}} P^1_{2s-3} \\
& + \sum_{l=0}^{\infty} [2(2l)(2l+2)(-\tau^{2l}_{2s} + (\beta_2)^{2l}_{2s} + (\gamma_2)^{2l}_{2s}) r^{2l-1} \\
& + 2(2l+1)(2l+3)(\xi^{2l}_{2s} + (\sigma_2)^{2l}_{2s}) r^{2l+1}] P^1_{2l+1}\Bigg\} \\
& + F_2 \frac{4r}{\beta}(-\tfrac{3}{5}P^1_1 + \tfrac{4}{15}P^1_3) + E_2 \frac{8r}{\beta}(-\tfrac{3}{5}P^1_1 + \tfrac{4}{15}P^1_3) \\
& + \sum_{s=1}^{\infty} E_{2s}\Bigg\{ -\frac{(2s+1)(2s-1)}{r^{2s+2}} P^1_{2s-1} \\
& + \sum_{l=0}^{\infty} [2(2l)(2l+2)(-\alpha^{2l}_{2s} + (\beta_1)^{2l}_{2s} + (\gamma_1)^{2l}_{2s}) r^{2l-1} \\
& + 2(2l+1)(2l+3)(\sigma_1)^{2l}_{2s} r^{2l+1}] P^1_{2l+1}\Bigg\} + 2Vr(-\tfrac{3}{5}P^1_1 + \tfrac{4}{15}P^1_3).
\end{aligned} \tag{4.4}$$

The pressure is related to ψ by (Happel & Brenner 1965, p. 121)

$$\frac{\partial p}{\partial r} = -\frac{1}{r^2 \sin\theta}\frac{\partial}{\partial \theta}(E^2\psi), \tag{4.5}$$

$$\frac{\partial p}{\partial \theta} = \frac{1}{\sin\theta}\frac{\partial}{\partial r}(E^2\psi), \tag{4.6}$$

where

$$E^2\psi = \frac{\partial^2 \psi}{\partial r^2} + \frac{\sin\theta}{r^2}\frac{\partial}{\partial \theta}\left(\frac{1}{\sin\theta}\frac{\partial \psi}{\partial \theta}\right). \tag{4.7}$$

After substituting (3.24) in (4.7), the pressure is obtained by integrating both (4.5) and (4.6). Comparing the two results, we find:

$$\begin{aligned}
p = \sum_{s=1}^{\infty} F_{2s}\Bigg\{ & -\frac{2s-1}{r^{2s}} P_{2s-1} + \sum_{l=0}^{\infty} (4l+4)(4l+5)(\xi^{2l}_{2s} + (\sigma_2)^{2l}_{2s}) r^{2l+1} P_{2l+1}\Bigg\} \\
& + \sum_{s=1}^{\infty} E_{2s}\Bigg\{ \sum_{l=0}^{\infty} (4l+4)(4l+5)(\sigma_1)^{2l}_{2s} r^{2l+1} P_{2l+1}\Bigg\} \\
& - 8F_2 \frac{r}{\beta} P_1 - 16E_2 \frac{r}{\beta} P_1 - 4VrP_1 + p_0,
\end{aligned} \tag{4.8}$$

where p_0 is an arbitrary constant pressure. The normal stress (4.3) is then

$$\tau_{rr} = \sum_{s=1}^{\infty} F_{2s}\left\{\frac{2s-1}{4s-3}\,\frac{(s-1)(4s+6)+3}{r^{2s}}\,P_{2s-1} - \frac{(2s-1)(2s-2)(2s-3)}{(4s-3)\,r^{2s}}\,P_{2s-3}\right.$$
$$+ \sum_{l=0}^{\infty}\left[2(2l+2)(2l+1)(2l)\left(-\tau_{2s}^{2l}+(\beta_2)_{2s}^{2l}+(\gamma_2)_{2s}^{2l}\right)r^{2l-1}\right.$$
$$\left.\left.+\,2(2l+2)(4l^2+2l-3)\left(\xi_{2s}^{2l}+(\sigma_2)_{2s}^{2l}\right)r^{2l+1}\right]P_{2l+1}\right\}$$
$$+ \sum_{s=1}^{\infty} E_{2s}\left\{\frac{(2s+1)(2s)(2s-1)}{r^{2s+2}}\,P_{2s-1}\right.$$
$$+ \sum_{l=0}^{\infty}\left[2(2l+2)(2l+1)(2l)\left(-\alpha_{2s}^{2l}+(\beta_1)_{2s}^{2l}+(\gamma_1)_{2s}^{2l}\right)r^{2l-1}\right.$$
$$\left.\left.+\,2(2l+2)(4l^2+2l-3)\,(\sigma_1)_{2s}^{2l}\,r^{2l+1}\right]P_{2l+1}\right\} + \frac{8F_2 r}{\beta}\left(\tfrac{3}{5}P_1+\tfrac{2}{5}P_3\right),$$
$$+\frac{16E_2 r}{\beta}\left(\tfrac{3}{5}P_1+\tfrac{2}{5}P_3\right)+4Vr\left(\tfrac{3}{5}P_1+\tfrac{2}{5}P_3\right)+p_0+gz\,\frac{a^3}{\nu^2}. \tag{4.9}$$

The stresses (4.4) and (4.9) are now substituted in (4.1). After performing the integration in (4.1), it is found that, although all the coefficients E_{2s} and F_{2s} enter due to $\tau_{r\theta}$ and τ_{rr} considered separately, the end result depends only on F_2. The result is

$$F_e + W_s - W_b - 4\pi F_2 = 0, \tag{4.10}$$

where $W_b = W_b'/\rho\nu^2$ and W_b' is the weight of the displaced fluid, i.e. the buoyant force. The difference $(W_s - W_b)$ is the submerged weight of the particle, W_f. The term $4\pi F_2$ is the viscous drag, D. Hence (4.10) may be written:

$$F_e + W_f = D = 4\pi F_2. \tag{4.11}$$

At this point, using (4.8) for the pressure, it is a simple matter to compute the pressure drop per sphere, Δp, defined by

$$\Delta p = [p]_{\substack{R=R_0\\ z=\frac{1}{2}\beta}} - [p]_{\substack{R=R_0\\ z=-\frac{1}{2}\beta}}, \tag{4.12}$$

where R_0 is any radius. From the cylindrical co-ordinate form of ψ, (3.3), (3.4) and (2.17), it may be shown that most of the terms in (4.8) are periodic in z and do not contribute to Δp. The end result is

$$\Delta p = -8F_2 - 16E_2 - 4V\beta. \tag{4.13}$$

A mean pressure gradient, p_z, is defined by

$$p_z = \frac{\Delta p}{\beta} = -\frac{8}{\beta}(F_2 + 2E_2) - 4V. \tag{4.14}$$

For Poiseuille flow having the same discharge, Q, as the present case, but without any spheres present, the pressure gradient will be denoted p_{z0}. In the present notation,

$$p_{z0} = -4V, \tag{4.15}$$

which is the last term of (4.14).

5. Numerical results

Computations were performed on the IBM 7094 computer system, first, to evaluate the coefficients E_{2s} and F_{2s}. Successively larger truncations of (3.27) and (3.28) were solved, until the values of E_{2s} and F_{2s} did not change by more than one place in the fifth significant figure of E_2 and F_2.

Values of the stream function, ψ, were computed next, using a grid of at least 25×25 points, from which streamlines were drawn by interpolation. Velocity distributions on two cross-sections were computed using (2.9) and (3.24). The stress distribution on the spheres, drag and pressure drop were computed using (4.4), (4.9), (4.11) and (4.13). Computations were carried out for arbitrary sphere velocity, U, and arbitrary discharge, $Q = \frac{1}{2}\pi V$. The results are reported for each of the three cases (i) $U \neq 0$, $V = 0$, (ii) $U = 0$, $V \neq 0$, (iii) zero drag.

Figures 2 and 3 show a typical set of streamlines for the case of $\beta = 1{\cdot}5$, $\lambda = 0{\cdot}5$. Figure 2(a) shows streamlines for the case of spheres moving in a fixed tube with zero discharge. Streamlines for the same flow, but viewed from the relative co-ordinate system fixed to the spheres, are shown in figure 2(b). Figure 2(c) shows streamlines for the case of flow with discharge $Q = \frac{1}{2}\pi V$ past fixed spheres in a fixed tube.

The streamline patterns in figure 2 are similar to those computed by Haberman & Sayre (1958) for a single sphere in an infinitely long tube. One new feature is the presence in figure 2(a) of a layer near the tube wall, which moves continuously in the negative z-direction. No such layer is present in the case of a single sphere.

Figure 3 shows streamlines for the case of zero drag on the spheres, which results when a mixture of neutrally bouyant spheres and fluid is pumped through the tube by a pressure gradient. Figure 3(a) shows the streamlines relative to the fixed tube wall. Figure 3(b) shows the same flow viewed in relative co-ordinates, which move with the spheres. The most striking feature of these curves is that, in figure 3(a), all streamlines are nearly straight lines. Since the spheres are rigid, this means that all the fluid within a cylinder having the same radius as that of the spheres moves almost as a rigid body. This pattern is closely approximated by the flow sometimes referred to as a 'stacked coins' flow (Whitmore 1967), in which a continuous, neutrally buoyant stack of disks moves along the axis of the tube surrounded by a concentric layer of fluid.

Figure 3(b) shows that the flow between spheres, when viewed in a co-ordinate system fixed to them, is a vortex motion similar to that computed by Brandt & Bugliarello (1965) in the spaces between disks, which extend to the full diameter of the tube.

The drag on each sphere is given by (4.11), in which the coefficient F_2 is in general of the form

$$F_2 = F_{2U}\, U + F_{2V}\, V, \tag{5.1}$$

where F_{2U} and F_{2V} are coefficients computed when E_{2s} and F_{2s} are found. In dimensional form, the drag D' is

$$D' = 6\pi\mu\lambda a(-K_U\, U' + K_V\, V'), \tag{5.2}$$

where

$$K_U = \frac{-2}{3\lambda} F_{2U}, \quad K_V = \frac{2}{3\lambda} F_{2V}. \tag{5.3}$$

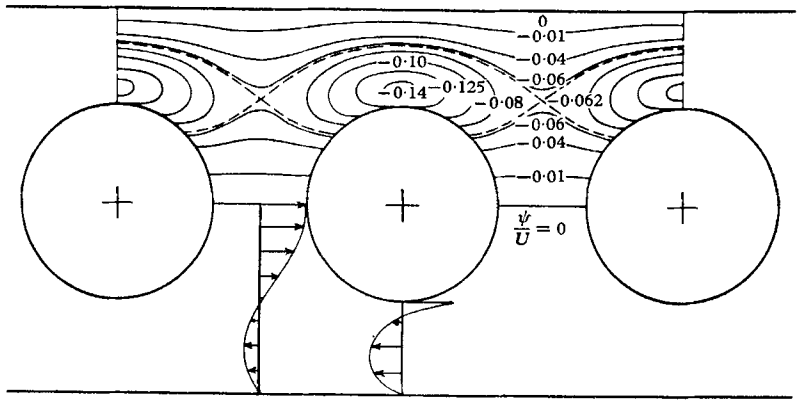

(*a*) $U \neq 0$, $V = 0$

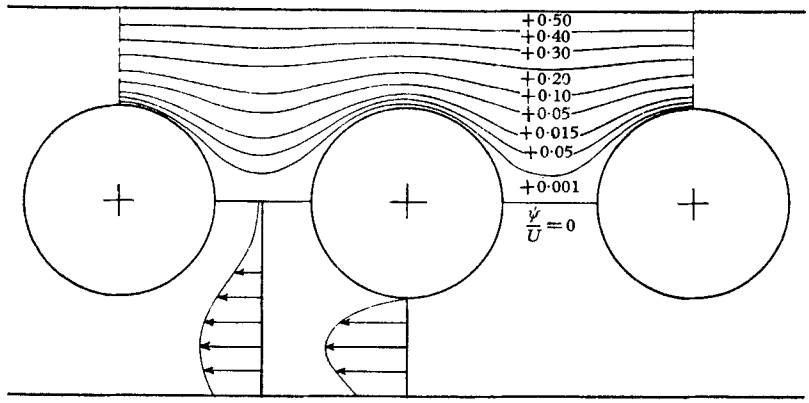

(*b*) $U \neq 0$, $V = 0$

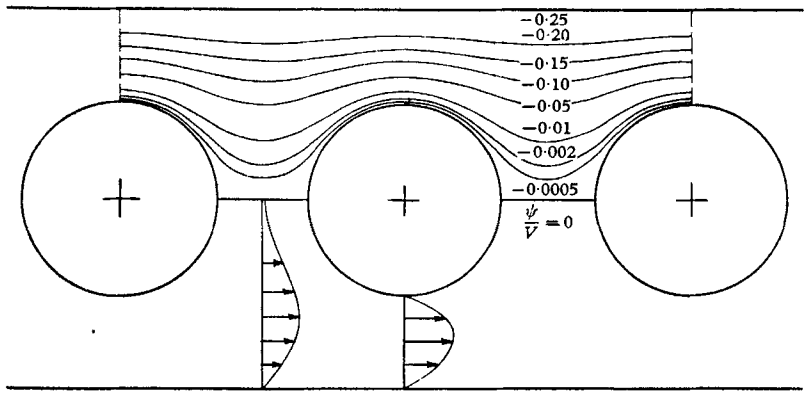

(*c*) $U = 0$, $V \neq 0$

FIGURE 2. Streamlines and velocity profiles for $\beta = 1{\cdot}5$, $\lambda = 0{\cdot}5$. (*a*) Spheres moving ($U \neq 0$, $V = 0$). Streamlines shown in co-ordinates fixed to the cylinder. (*b*) Spheres moving ($U \neq 0$, $V = 0$). Streamlines shown in co-ordinates moving with the spheres. (*c*) Spheres and cylinder fixed ($U = 0$, $V \neq 0$). Streamlines shown for discharge $Q = \frac{1}{2}\pi V$.

The drag on a single sphere moving with a velocity U' in an infinite fluid whose velocity is V' at infinity is Stokes's drag,

$$D' = 6\pi\mu\lambda a(-U' + V'). \tag{5.4}$$

K_U and K_V in (5.2) are normalized drag coefficients equal to unity for Stokes's drag.

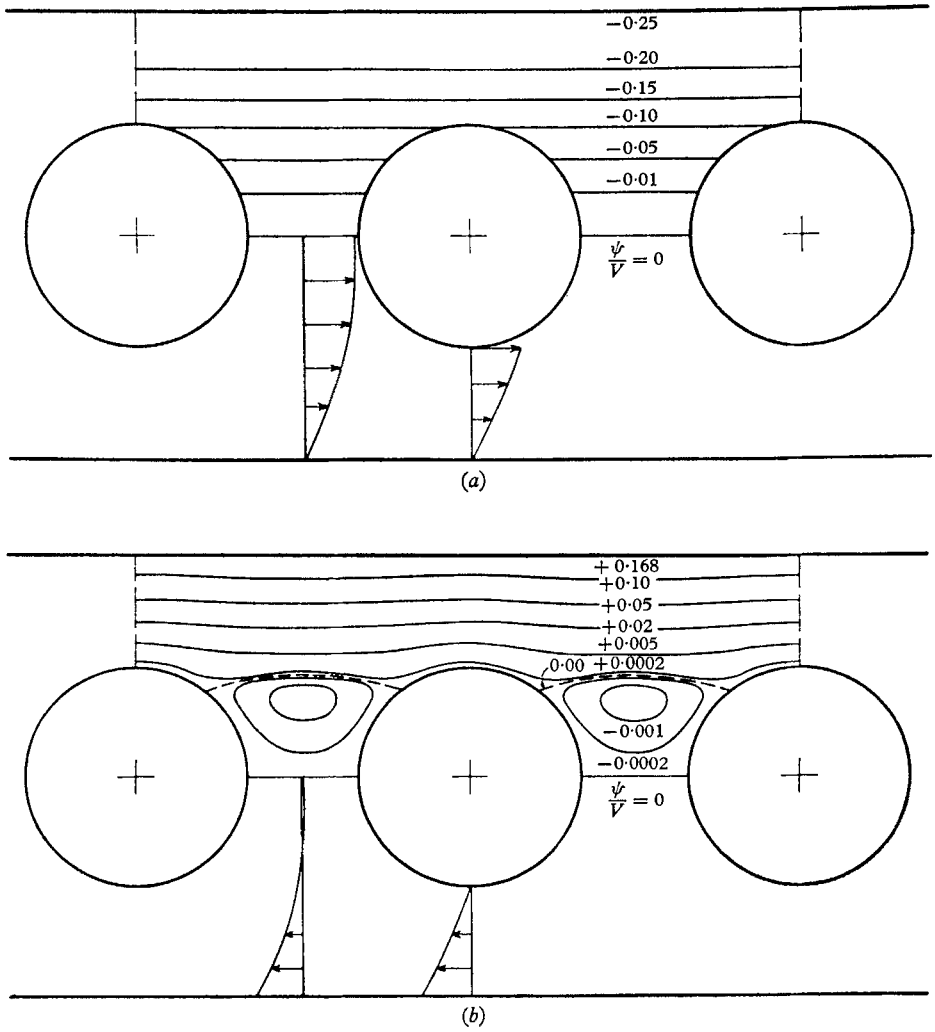

FIGURE 3. Streamlines and velocity profiles for $\beta = 1{\cdot}5$, $\lambda = 0{\cdot}5$, zero drag case. (*a*) Streamlines shown in co-ordinates fixed to the cylinder. (*b*) Streamlines shown in co-ordinates moving with the spheres.

Table 1 gives the coefficients K_U computed for a line of spheres, except the last column, which contains values for a single sphere given by Haberman & Sayre (1958). The results of the present computations for $\beta = 40$ agree with those of Haberman & Sayre (which correspond to $\beta = \infty$) to three or four significant figures for most cases.

λ	$\beta = 2\lambda$	$\beta = 1{\cdot}0$	$\beta = 1{\cdot}4$	$\beta = 2{\cdot}0$	$\beta = 4{\cdot}0$	$\beta = 40$	Haberman & Sayre
0·1	0·473	1·225	1·258	1·263	1·263	1·263	1·263
0·2	0·8721	1·559	1·660	1·679	1·680	1·680	1·680
0·3	1·531	2·096	2·317	2·368	2·370	2·370	2·371
0·4	2·719	3·075	3·463	3·585	3·591	3·592	3·596
0·5	5·042	5·042	5·675	5·929	5·947	5·949	5·970
0·6	10·14	—	10·56	11·04	11·09	11·10	11·14
0·7	23·60	—	23·60	24·52	24·67	24·70	24·96
0·8	72·69	—	—	73·90	74·60	74·97	73·56
0·9	430·0	—	—	440·0	460·0	—	—

TABLE 1. Drag coefficient, K_U

λ	$\beta = 2\lambda$	$\beta = 1{\cdot}0$	$\beta = 1{\cdot}4$	$\beta = 2{\cdot}0$	$\beta = 4{\cdot}0$	$\beta = 40$	Haberman & Sayre
0·1	0·469	1·216	1·249	1·255	1·255	1·255	1·255
0·2	0·8433	1·517	1·616	1·634	·1635	1·635	1·635
0·3	1·422	1·964	2·177	2·227	2·229	2·229	2·231
0·4	2·393	2·723	3·092	3·210	3·216	3·216	3·218
0·5	4·158	4·158	4·735	4·977	4·995	4·996	5·004
0·6	7·750	—	8·121	8·562	8·613	8·617	8·651
0·7	16·54	—	16·54	17·34	17·47	17·49	17·67
0·8	46·12	—	—	47·06	47·58	47·81	47·30
0·9	250·0	—	—	250·0	260·0	—	—

TABLE 2. Drag coefficient, K_V

λ	$\beta = 2\lambda$	$\beta = 1{\cdot}0$	$\beta = 1{\cdot}4$	$\beta = 2{\cdot}0$	$\beta = 4{\cdot}0$	$\beta = 40$
0·1	1·983	1·987	1·987	1·987	1·987	1·987
0·2	1·934	1·944	1·947	1·947	1·947	1·947
0·3	1·857	1·873	1·879	1·881	1·881	1·881
0·4	1·760	1·771	1·786	1·791	1·791	1·791
0·5	1·649	1·649	1·669	1·679	1·680	1·680
0·6	1·528	—	1·538	1·551	1·553	1·553
0·7	1·401	—	1·401	1·414	1·416	1·416
0·8	1·271	—	—	1·274	1·276	1·276
0·9	1·14	—	—	1·14	1·14	—

TABLE 3. Ratio of $2U/V$ for zero drag

							Happel & Byrne	
λ	$\beta = 2\lambda$	$\beta = 1{\cdot}0$	$\beta = 1{\cdot}4$	$\beta = 2{\cdot}0$	$\beta = 4{\cdot}0$	$\beta = 40{\cdot}0$	$\beta = 1{\cdot}4$	$\beta = 40{\cdot}0$
0·1	0·558	1·450	1·488	1·496	1·496	1·496	1·489	1·496
0·2	1·959	3·543	3·776	3·821	3·822	3·822	3·774	3·819
0·3	4·769	6·641	7·384	7·560	7·566	7·566	7·367	7·543
0·4	10·18	11·65	13·33	13·88	13·90	13·91	13·26	13·79
0·5	20·77	20·77	23·94	25·33	25·43	25·44	23·68	24·98
0·6	43·18	—	45·54	48·49	48·84	48·86	44·44	47·15
0·7	98·62	—	98·62	104·5	105·6	105·7	93·21	98·94
0·8	283·9	—	—	291·3	295·2	296·6	—	263·1
0·9	1500	—	—	1500	1600	—	—	—

TABLE 4. Pressure drop coefficient, P_V

The effect of neighbouring spheres on the drag exerted on each sphere is small, if the spacing is greater than about one tube diameter ($\beta > 2$). The data in table 1 are plotted in figure 4. It is seen that, the closer the spheres, the less becomes the drag per sphere. For large spheres, the effect of spacing is less pronounced. Table 2 and figure 5 show similar results for K_V; the qualitative results are the same as for K_U.

							Happel & Byrne	
λ	$\beta = 2\lambda$	$\beta = 1{\cdot}0$	$\beta = 1{\cdot}4$	$\beta = 2{\cdot}0$	$\beta = 4{\cdot}0$	$\beta = 40$	$\beta = 1{\cdot}4$	$\beta = 40$
0·1	0·563	1·460	1·499	1·506	1·506	1·506	1·499	1·506
0·2	2·024	3·640	3·877	3·922	3·924	3·924	3·877	3·923
0·3	5·118	7·069	7·837	8·018	8·024	8·025	7·839	8·021
0·4	11·49	13·07	14·84	15·41	15·44	15·44	14·85	15·40
0·5	24·95	24·95	28·41	29·86	29·97	29·98	28·38	29·74
0·6	55·80	—	58·47	61·65	62·01	62·04	57·80	60·72
0·7	138·9	—	138·9	145·6	146·8	147·0	133·0	139·7
0·8	442·8	—	—	451·7	456·8	459·0	—	412·7
0·9	2700	—	—	2700	2800	—	—	—

TABLE 5. Pressure drop coefficient, P_U

λ	$\beta = 2\lambda$	$\beta = 1{\cdot}0$	$\beta = 1{\cdot}4$	$\beta = 2{\cdot}0$	$\beta = 4{\cdot}0$	$\beta = 40{\cdot}0$
0·1	$0{\cdot}730 \times 10^{-4}$	$0{\cdot}1995 \times 10^{-4}$	$0{\cdot}1427 \times 10^{-4}$	$0{\cdot}1016 \times 10^{-4}$	$0{\cdot}501 \times 10^{-5}$	$0{\cdot}501 \times 10^{-6}$
0·2	$0{\cdot}1199 \times 10^{-2}$	$0{\cdot}6347 \times 10^{-3}$	$0{\cdot}453 \times 10^{-3}$	$0{\cdot}320 \times 10^{-3}$	$0{\cdot}160 \times 10^{-3}$	$0{\cdot}166 \times 10^{-4}$
0·3	$0{\cdot}6177 \times 10^{-2}$	$0{\cdot}4617 \times 10^{-2}$	$0{\cdot}3451 \times 10^{-2}$	$0{\cdot}2438 \times 10^{-2}$	$0{\cdot}1220 \times 10^{-2}$	$0{\cdot}1220 \times 10^{-3}$
0·4	0·01953	0·01775	0·01430	$0{\cdot}999 \times 10^{-2}$	$0{\cdot}5199 \times 10^{-2}$	$0{\cdot}5199 \times 10^{-3}$
0·5	0·04933	0·04933	0·04245	0·03235	0·01631	0·001631
0·6	0·112	—	0·1039	0·0840	0·0428	0·00429
0·7	0·234	—	0·2339	0·1961	0·103	0·0103
0·8	0·500	—	—	0·455	0·242	0·0243
0·9	1·3	—	—	1·2	0·64	—

TABLE 6. Pressure gradient coefficient, G_{V0}, for zero drag

The above results are utilized for the case of zero drag for neutrally buoyant spheres by setting D' (5.2) equal to zero, and solving for U in terms of V. The ratio $2U/V$ is the ratio of the velocity of the spheres to the mean flow velocity of the mixture. Numerical values are given in table 3. Small spheres travel at nearly twice the mean velocity, but as λ increases the sphere velocity approaches the mean velocity from above.

The pressure drop per sphere and the pressure gradient are given, in general, by (4.13) and (4.14), in which F_2 and E_2 are each linear in U and in V. Hence, in dimensional form, the total pressure drop per sphere may be written

$$\Delta p' = \frac{\mu}{a}(-V'P_V + U'P_U) - \frac{4\mu V'}{a}\beta + \rho g \beta a; \tag{5.5}$$

and the total pressure gradient in dimensional form may be written:

$$p'_z = \frac{4\mu}{a^2}(-V'G_V + U'G_U) - \frac{4\mu V'}{a^2} + \rho g, \tag{5.6}$$

where P_V, P_U, G_V and G_U are coefficients derived from the E_2 and F_2 values computed previously. The term $(4\mu V'/a^2)$ in (5.6) is the Poiseuille flow pressure gradient; likewise, the term $(4\mu V'\beta/a)$ in (5.5) is the pressure drop in a length βa in Poiseuille flow. The terms involving g are the hydrostatic effects. Hence, in (5.6), the coefficients G_V and G_U are a measure of the additional pressure gradient due to the presence of the spheres. Similarly, P_V and P_U are a measure of the additional pressure drop, due to the spheres, in a length βa.

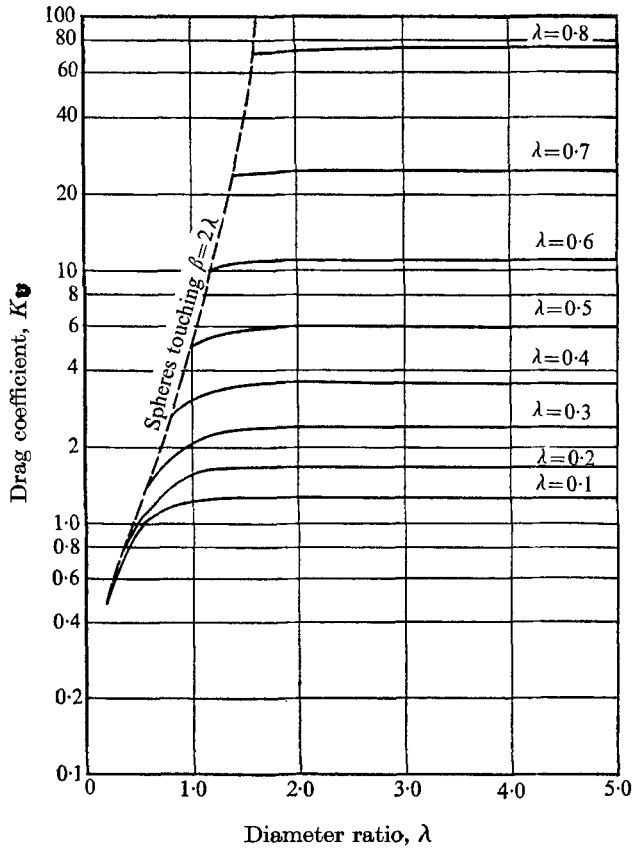

FIGURE 4. Drag coefficient, K_U.

Table 4 gives the pressure drop coefficient P_V. The last two columns are the results computed from the following approximate formula, which is given by Happel & Byrne (1954):

$$\Delta p'_a = \frac{2D'}{\pi a^2}[1 - \tfrac{2}{3}\lambda^2]. \tag{5.7}$$

The last two columns of table 4 are computed using (5.7), with the drag D' based on the coefficients in table 2. The approximate results are good for $\lambda \leqslant 0{\cdot}5$.

Table 5 gives the computed values of P_U. Figures 6 and 7 show $(1+P_V)$ and $(1+P_U)$ as functions of λ. It may be seen that the qualitative trends in the pressure drop coefficients are the same as for the drag coefficients discussed above.

In the case of zero drag, U depends on V, as shown in table 3. Hence in dimensional form the pressure gradient may be written

$$p'_z = \frac{4\mu}{a^2}(-V'G_{V0}) - \frac{4\mu V'}{a^2} + \rho g, \tag{5.8}$$

where G_{V0} is a coefficient which is a measure of the additional pressure gradient due to the presence of the spheres compared to that for Poiseuille flow having the same discharge. Numerical values of G_{V0} are given in table 6 and plotted

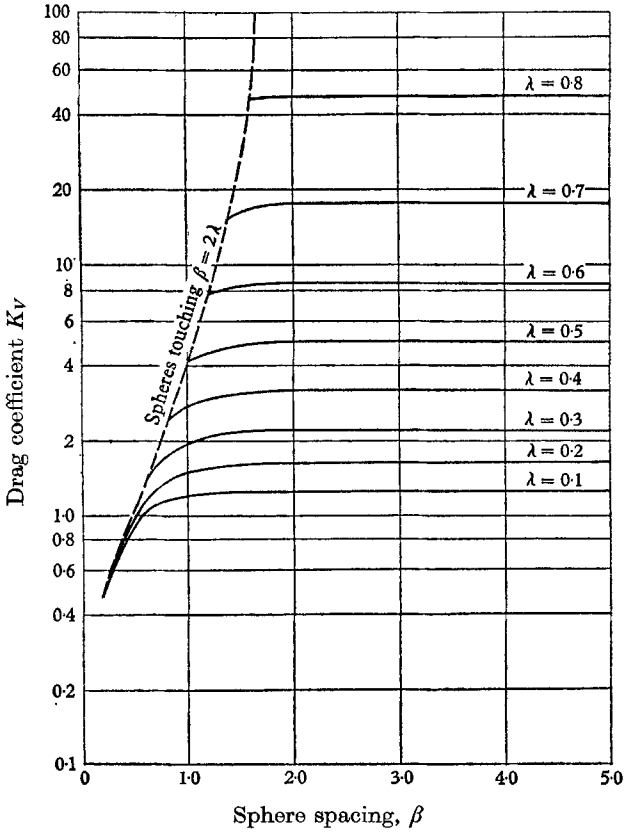

FIGURE 5. Drag coefficient, K_V.

in figure 8. These show that the additional pressure gradient is generally small, and is less than 50% over that for Poiseuille flow for λ less than 0·8. The upper curve in figure 8 shows the comparable coefficient, G_{V0}, for the stacked coins model (Whitmore 1967), which in the present termnology is

$$G_{V0} = \frac{\lambda^4}{1-\lambda^4}. \tag{5.9}$$

The results show that the additional pressure drop for the case of spheres touching is about 75% of that for the stacked coins model, when the coins and spheres have the same diameter.

The additional pressure drop per sphere in the zero drag case is

$$\Delta p' = -\frac{\mu}{a} V' P_{V0}, \tag{5.10}$$

where values of the coefficient P_{V0} are given in table 7. Again, there is little interaction between spheres for $\beta > 2$.

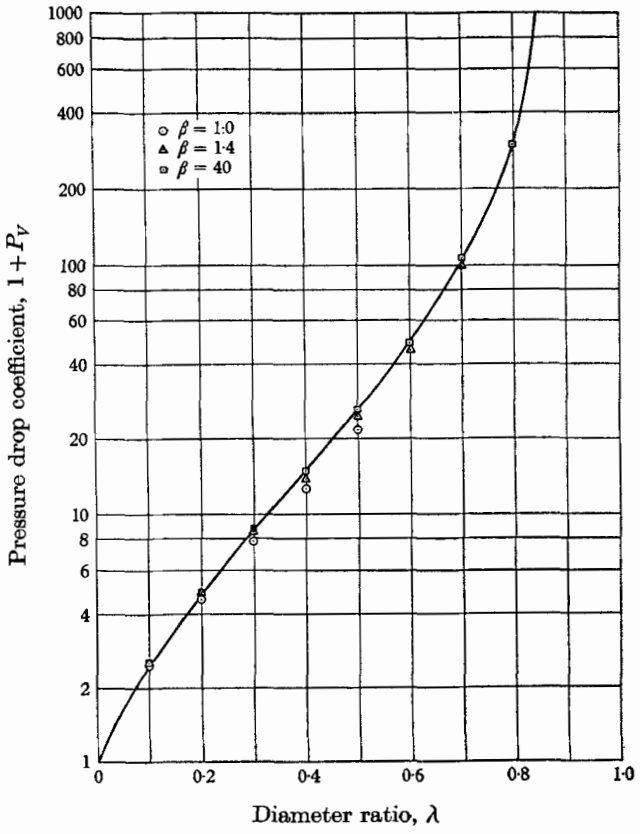

FIGURE 6. Pressure drop coefficient, $1+P_V$.

λ	$\beta = 2\lambda$	$\beta = 1{\cdot}0$	$\beta = 1{\cdot}4$	$\beta = 2{\cdot}0$	$\beta = 4{\cdot}0$	$\beta = 40{\cdot}0$
0·1	$0{\cdot}584 \times 10^{-4}$	$0{\cdot}789 \times 10^{-4}$	$0{\cdot}799 \times 10^{-4}$	$0{\cdot}800 \times 10^{-4}$	$0{\cdot}801 \times 10^{-4}$	$0{\cdot}801 \times 10^{-4}$
0·2	$0{\cdot}1919 \times 10^{-2}$	$0{\cdot}2359 \times 10^{-2}$	$0{\cdot}2559 \times 10^{-2}$	$0{\cdot}2562 \times 10^{-2}$	$0{\cdot}2562 \times 10^{-2}$	$0{\cdot}2562 \times 10^{-2}$
0·3	0·01482	0·01847	0·01932	0·01951	0·01951	0·01951
0·4	0·06249	0·07100	0·08010	0·08296	0·08318	0·08319
0·5	0·1973	0·1973	0·2377	0·2588	0·2609	0·2609
0·6	0·537	—	0·582	0·672	0·685	0·687
0·7	1·310	—	1·31	1·57	1·65	1·65
0·8	3·20	—	—	3·64	3·81	3·9
0·9	9·3	—	—	9·6	10·0	—

TABLE 7. Pressure drop coefficient, P_{V0}, for zero drag

The results above have been developed and presented as if the particle velocity, U, and fluid discharge, Q (or V), were given and the drag and pressure drop were to be found. The results above may also be used to find U and Q for particles of given size, spacing and density, assuming that the fluid properties, gravitational constant, pressure gradient and applied external force are also given. From the tabulated results and the particle size and spacing, the coefficients

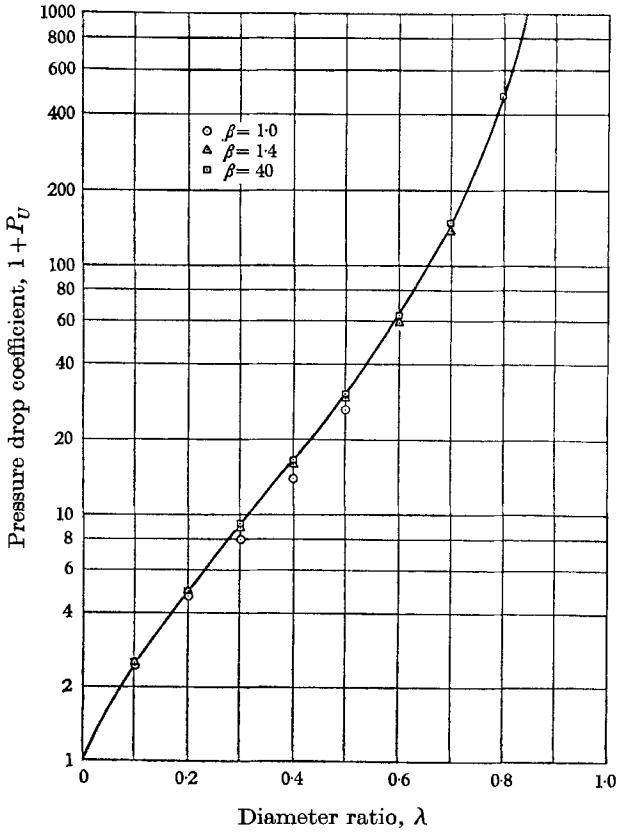

FIGURE 7. Pressure drop coefficient, $1+P_U$.

K_U, K_V in (5.2), and G_U, G_V in (5.6), may be determined. Then, equating the drag in (5.2) to the known applied external force and the weight of the particle in fluid, and substituting the known pressure gradient in (5.6), gives a pair of equations, which may be solved for U and V.

6. Conclusion

With respect to the problem of capillary blood flow, the present study suggests two general conclusions. First, if the particles (red blood cells) are spaced more than one tube diameter apart, their interaction is negligible. Secondly, if the tube diameter is at least 20 % greater than the particle diameter, the additional

pressure drop will not be greater than about 50 % of the Poiseuille pressure drop of the suspending medium (blood plasma) alone. This is an interesting conclusion, because the viscosity of blood is generally at least twice that of the plasma alone in shear viscometer tests and in large tubes (Gregersen 1967). This corroborates experimental measurements in fine tubes (Haynes 1961), which show that the effective viscosity of blood is less in capillaries than in larger vessels.

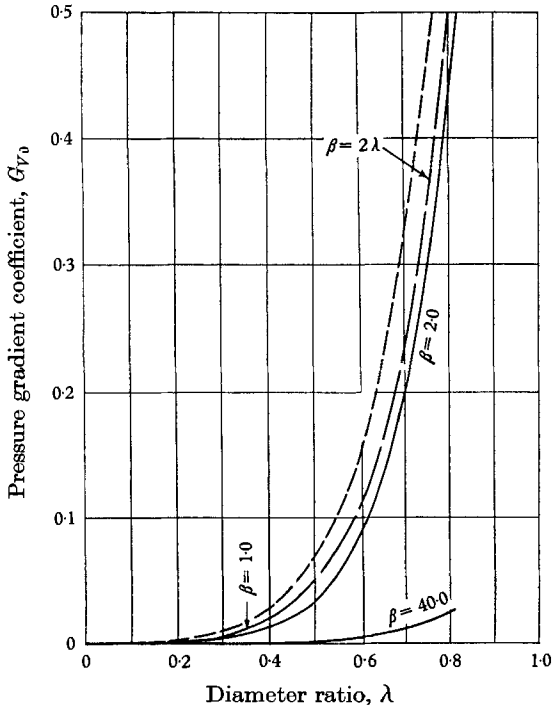

FIGURE 8. Pressure gradient coefficient, G_{V_0}, for the case of zero drag. Solid curves are computed results for a line of spheres. Dotted curve is for the stacked coins model. Dashed curve ($\beta = 2\lambda$) is for a line of spheres which are touching.

This paper was based on Wang (1967). The work was supported by the Office of Naval Research, Project NR 062–393.

REFERENCES

ATSUMI, A. 1960 *J. Appl. Mech.* **82E**, 87–92.

BRANDT, A. & BUGLIARELLO, G. 1965 *Annual Conf. on Engineering in Med. and Biol.* **7**, 159.

GREGERSEN, M. I. 1967 *Colloque International organisé pour la circulation, Paris.* Masson et Cie, pp. 231–244.

HABERMAN, W. L. & SAYRE, R. M. 1958 *David Taylor Model Basin Report* 1143. Washington, D.C.

HAPPEL, J. & BRENNER, H. 1965 *Low Reynolds Number Hydrodynamics.* New Jersey: Prentice-Hall.

HAPPEL, J. & BYRNE, B. J. 1954 *Ind. Engng Chem.* **46**, 1181–1186.

HAYNES, R. H. 1961 *Trans. Soc. Rheol.* **5**, 85–101.

HOBSON, E. W. 1955 *The Theory of Spherical and Ellipsoidal Harmonics*. New York: Chelsea.

LIGHTHILL, M. J. 1968 *J. Fluid Mech.* **34**, 113.

LING, C. B. 1963 *The Collected Papers of C. B. Ling*. Taipei: Academia Sinica.

MACROBERT, T. M. 1948 *Spherical Harmonics*. New York: Dover.

SONSHINE, R. M. & BRENNER, H. 1966 *Appl. Sci. Res.* **16**, 425–454.

WANG, H. 1967 Ph.D. Thesis, Columbia University.

WANG, H. & SKALAK, R. 1967 *Tech. Rept.* 1, *Project NR* 062–393. New York: Colombia University.

WATSON, G. N. 1944 *Theory of Bessel Functions*. Cambridge University Press.

WHITMORE, R. L. 1967 *Proc. Int. Conf. on Hemorheology* (Copley, ed.). Oxford: Pergamon.